On Accuracy of Perfect Electric Conductor Implementation in Lebedev FDTD

Mahbod Salmasi, *Student Member, IEEE*, M. E. Potter, *Senior Member, IEEE*, and Michal Okoniewski, *Fellow, IEEE*

***Abstract*—The Lebedev grid is an alternative to Yee grid where, because the discretized fields lie at the same location in space, there is no need for further field interpolations when modeling anisotropic materials. In this letter, we focus on accurately implementing perfect electric conductors with planar interfaces, as well as 90° and 270° corners. Simulations are provided to demonstrate the overall improvements and also the second-order accuracy of the proposed methods.**

***Index Terms*—Finite-difference time-domain (FDTD), finite-difference methods.**

I. Introduction

THE original Yee finite-difference time-domain (FDTD) method [1] is not particularly well suited to modeling anisotropic materials. With off-diagonal anisotropy, spatial derivatives in all directions are needed at the same location for the discrete field updates, which are not immediately available because of the assumed grid. Instead, most anisotropic FDTD implementations interpolate from nearby field components [2]. However, this inherently introduces further error and makes dealing with material interfaces more complicated as a larger computational stencil is needed. Moreover, it may cause late-time instabilities. As discussed in [3], stability requires that the operation of interpolation combined with the inverse permittivity matrix be symmetric and positive definite (in fact, for all numerical implementations of the constitutive relations).

The Lebedev-FDTD method was previously introduced in [4] and [5] as an alternative for handling simulations with anisotropic material. It is well suited for that as field components are collocated.

In this letter, we focus our attention on perfect electric conductor (PEC) boundary conditions in Lebedev grid, as Liu *et al.* [5] do not mention how they implement PEC boundaries, and Nauta *et al.* [4] use image theory to implement planar PEC interfaces and 90° corners, but the method is inaccurate. Here, we propose an alternative implementation of PEC boundaries that is more accurate and can be extended to 90° as well as 270° corners. To demonstrate the accuracy of the proposed method, rectangular and ridged resonators and a parallel-plate waveguide will be simulated to encompass different types of PEC interfaces.

Manuscript received December 22, 2017; accepted January 10, 2018. Date of publication January 15, 2018; date of current version March 1, 2018. This work was supported in part by the Natural Sciences and Engineering Research Council of Canada under Grant No. RGPIN/03984-2014. *(Corresponding author: Mike Potter.)*

The authors are with the Department of Electrical and Computer Engineering, Schulich School of Engineering, University of Calgary, Calgary, AB T2N 1N4, Canada (e-mail: mahbod.salmasi@ucalgary.ca; mpotter@ucalgary.ca; okoniews@ucalgary.ca).

Digital Object Identifier 10.1109/LAWP.2018.2794206

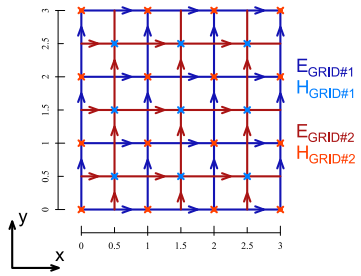

Fig. 1. Lebedev grid in two dimensions for TE_z polarization.

Also, the order of the accuracy for the Lebedev method is investigated in the presence of PEC boundaries, to complement the investigation into its accuracy with open boundaries [6].

In what follows, the Lebedev method is briefly described, followed by handling of PEC interfaces. A rectangular resonator filled with anisotropic material, and then a parallel-plate waveguide filled with anisotropy, for which we also present analytical solutions, will be simulated. Finally, a ridged resonator is simulated to cover 270° as well.

II. Lebedev Grid

The Lebedev grid is a cubic tessellation of three-dimensional (3-D) space similar to the Yee grid, but with collocated field components; magnetic and electric fields are located at different places in space however. Lebedev grid can be thought of as four Yee grids shifted with respect to each other in two of the three *x*-, *y*-, and *z*-directions [4]. In two dimensions, Lebedev grid consists of only two shifted Yee grids instead of four. A TE_z configuration is shown in Fig. 1. The true advantage of the Lebedev method is revealed when the constitutive relationships have off-diagonal elements causing the two Yee building blocks of Lebedev to couple to each other. Otherwise, in regions of isotropic medium or one with diagonal anisotropy, the two Yee meshes are not coupled to each other at all. The locations of the fields on the Lebedev grid can be described by two sets of indices: $i, i', j,$ and j' are chosen from the set of numbers $\{0, \frac{1}{2}, 1, \frac{3}{2}, \ldots\}$ such that $2(i+j)$ is an odd and $2(i'+j')$ is an even number. The update equations are then

$$\begin{bmatrix} E_x^{+1}(i,j) \\ E_y^{+1}(i,j) \end{bmatrix} = \begin{bmatrix} E_x^{+0}(i,j) \\ E_y^{+0}(i,j) \end{bmatrix} + \frac{\bar{\bar{\epsilon}}_r^{-1}(i,j)\Delta t}{\epsilon_0} \begin{bmatrix} \frac{H_z^{\frac{1}{2}}\left(i,j+\frac{1}{2}\right) - H_z^{\frac{1}{2}}\left(i,j-\frac{1}{2}\right)}{\Delta y} \\ \frac{H_z^{\frac{1}{2}}\left(i-\frac{1}{2},j\right) - H_z^{\frac{1}{2}}\left(i+\frac{1}{2},j\right)}{\Delta x} \end{bmatrix} \quad (1)$$

$$H_z^{+\frac{1}{2}}(i',j') = H_z^{-\frac{1}{2}}(i',j') - \frac{\mu_r^{-1}(i',j')\Delta t}{\mu_0} \times \left[\frac{E_y^{+0}\left(i'+\frac{1}{2},j'\right) - E_y^{+0}\left(i'-\frac{1}{2},j'\right)}{\Delta x} + \frac{E_x^{+0}\left(i',j'-\frac{1}{2}\right) - E_x^{+0}\left(i',j'+\frac{1}{2}\right)}{\Delta y} \right] \quad (2)$$

where

$$\bar{\bar{\epsilon}}_r^{-1} = \begin{bmatrix} \left(\epsilon_r^{-1}\right)_{xx} & \left(\epsilon_r^{-1}\right)_{xy} \\ \left(\epsilon_r^{-1}\right)_{yx} & \left(\epsilon_r^{-1}\right)_{yy} \end{bmatrix}. \quad (3)$$

The update equations in the Lebedev method are closely related to its Yee counterpart. The magnetic update equation is actually the same (in two-dimensions). The electric field update equation is slightly different; it has both the *x*- and *y*-components of the curl of *H* at the same location that are then multiplied by the inverse permittivity matrix to contribute to the updated electric field value. Note that in (1), one of the electric fields resides on Grid #1, while the other component lies on Grid #2 (see Fig. 1). As can be observed, no additional interpolation is needed for the implementation of anisotropy. In a sense, the Lebedev technique runs two parallel Yee simulations simultaneously, both of which aim to simulate exactly the same problem but are shifted half a unit cell in space in order to get the other component of the curl of *H* at the same location in space.

III. Planar Boundaries

A. Previous Implementation

In the standard Yee method, PECs are realized by merely setting the tangential components of the electric field to the PEC interface to zero. In the Lebedev method, however, both tangential and normal field components lie on the interface. In the original Lebedev FDTD paper [4], image theory was used for implementing PECs along with the boundary conditions

$$\vec{E} \times \hat{n} = 0 \quad (4)$$

$$\partial\vec{D}/\partial n \cdot \hat{n} = 0 \quad (5)$$

$$\partial\vec{H}/\partial n \times \hat{n} = 0 \quad (6)$$

$$\vec{B} \cdot \hat{n} = 0 \quad (7)$$

where $\hat{n}$ is the unit vector normal to the PEC surface. The antisymmetry of the tangential electric fields and the symmetry of the tangential magnetic fields at the PEC interface are revealed. However, these boundary conditions are valid only for the electrostatic and magnetostatic case with anisotropic materials. Assume an interface of some anisotropic medium with PEC that has the normal unit vector $\hat{n} = \hat{y}$ as in Fig. 2. In this case, writing out Maxwell's equation for the tangential electric flux at the interface, knowing that the tangential electric field is zero, yields

$$\frac{\partial D_x}{\partial t} = \frac{\partial\left(\epsilon_{xx}E_x + \epsilon_{xy}E_y\right)}{\partial t} = \frac{\partial\left(\epsilon_{xy}E_y\right)}{\partial t} = \frac{\partial H_z}{\partial y} \neq 0 \quad (8)$$

which is not in agreement with the boundary condition (6) used in [4], resulting in errors being introduced in the previous

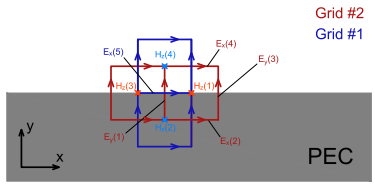

Fig. 2. Planar PEC boundary.

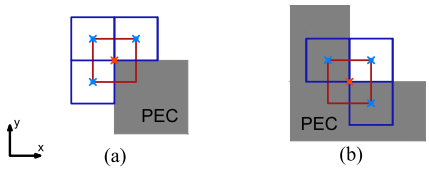

Fig. 3. Illustration of (a) 270° and (b) 90° corners.

implementation.[1] In the approach used in [4], (4) implies that we should mirror the electric fields behind the PEC wall, and (6) implies that we should mirror the magnetic fields before performing normal field updates. The second step, mirroring the magnetic fields, was originally equivalent to (incorrectly) inverting the permittivity tensor and then setting the off-diagonal elements to zero; we present this tensor modification for future reference as follows:

$$\bar{\bar{\epsilon}}_r^{-1} : \begin{bmatrix} \left(\epsilon_r^{-1}\right)_{xx} & \left(\epsilon_r^{-1}\right)_{xy} \\ \left(\epsilon_r^{-1}\right)_{yx} & \left(\epsilon_r^{-1}\right)_{yy} \end{bmatrix} \rightarrow \begin{bmatrix} \left(\epsilon_r^{-1}\right)_{xx} & 0 \\ 0 & \left(\epsilon_r^{-1}\right)_{yy} \end{bmatrix}. \quad (9)$$

B. Proposed Implementation

In our proposed method, we eliminated mirroring the electric fields in the first step by using CP-FDTD [8], [9], which simplifies exactly to the update equations derived from mirroring the electric fields in 90° corners and planar cases, but it also generalizes to 270° corners nicely (see Fig. 3), something that is not possible with image theory. The CP-FDTD update equation is expressed as

$$H_z^{+\frac{1}{2}} = H_z^{-\frac{1}{2}} - \frac{\mu_r^{-1}\Delta t}{\mu_0 S_c}\sum_{i=1}^{4} l_i E_i \quad (10)$$

where S_c is the area of the conformed cell, and l_i are lengths of the corresponding electric edges with sign appropriate to the direction of the edge. The magnetic update equation for the planar interface (see Fig. 2) now becomes

$$H_z^{+\frac{1}{2}}(1) = H_z^{-\frac{1}{2}}(1) - \frac{\mu_r^{-1}\Delta t}{\mu_0 \frac{1}{2}\Delta x\Delta y} \times \left(0E_x^{+0}(2) - \Delta x E_x^{+0}(4) + \frac{1}{2}\Delta y E_y^{+0}(3) - \frac{1}{2}\Delta y E_y^{+0}(1)\right).$$

In the same manner, the magnetic field update equations can be found easily for 90° and 270° corners by replacing the appropriate S_c and l_i. Now the correct form of updating normal

[1] It is also interesting to know that at dc frequency in the presence of anisotropic material with off-diagonal elements, a modified image theory [7], which is a skewed version of the standard one, must be used at distances away from the interface. However, in the previous method, not using the modified image theory does not introduce errors since we are very close to the interface.

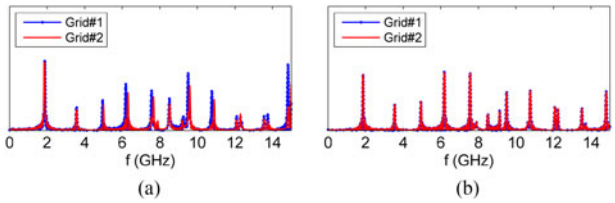

Fig. 4. Resonant frequencies of a rectangular resonator filled with anisotropic material: (a) method described in [4]; (b) proposed method.

component of the electric field is as follows:

$$\begin{bmatrix} \epsilon_{xx} & \epsilon_{xy} \\ \epsilon_{yx} & \epsilon_{yy} \end{bmatrix} \begin{bmatrix} 0 \\ E_y^{+1} \end{bmatrix} = \begin{bmatrix} \epsilon_{xx} & \epsilon_{xy} \\ \epsilon_{yx} & \epsilon_{yy} \end{bmatrix} \begin{bmatrix} 0 \\ E_y^{+0} \end{bmatrix} + \frac{\Delta t}{\epsilon_0} \begin{bmatrix} (\nabla \times H)_x \\ (\nabla \times H)_y \end{bmatrix}$$

resulting in

$$\epsilon_{yy} E_y^{+1} = \epsilon_{yy} E_y^{+0} + \frac{\Delta t}{\epsilon_0} (\nabla \times H)_y . \tag{11}$$

In general, the update equations for all types of interfaces can be handled by first zeroing the off-diagonal elements and then inverting the permittivity tensor:

$$\bar{\bar{\epsilon}}_r^{-1} : \begin{bmatrix} \left(\epsilon_r^{-1}\right)_{xx} & \left(\epsilon_r^{-1}\right)_{xy} \\ \left(\epsilon_r^{-1}\right)_{yx} & \left(\epsilon_r^{-1}\right)_{yy} \end{bmatrix} \rightarrow \begin{bmatrix} \left(\epsilon_{r_{xx}}\right)^{-1} & 0 \\ 0 & \left(\epsilon_{r_{yy}}\right)^{-1} \end{bmatrix} \tag{12}$$

as a correction to (9), as well as setting tangential electric fields to zero as necessary in the update.

IV. Validation Examples

In the following sections, examples are provided that demonstrate the improvement to PEC handling in the Lebedev method, as well as the methodology for handling PEC corners. In each case, Ansoft HFSS simulations are utilized as a comparison basis with the simulations running until relative frequency difference between runs is below 0.01%.

A. Rectangular Resonator Filled With Anisotropic Material

Since the 2-D Lebedev grid consists of two Yee grids, resonant frequency observations should be identical since the grids are simulating the same problem. To test this, a rectangular resonator of size 30 mm × 15 mm completely filled with material described by

$$\bar{\bar{\epsilon}}_r = \begin{bmatrix} 4 & 4 \\ 4 & 7 \end{bmatrix}$$

is simulated at 0.99 S, where S is the courant limit of the Yee method in free space. The cell sizes are chosen to be $\Delta x = \Delta y = 0.25$ mm. The excitation is the first derivative of a Gaussian pulse. For the Lebedev grid, a distributed weighted source instead of a point source must be used to excite both grids [4]. Here, we excited one single magnetic node on Grid#1 along with the four neighboring magnetic nodes on Grid#2 with quarter-weight. Also, to sample the fields for the Fourier transform, a single magnetic node on Grid#1 and the average of four of the neighboring magnetic nodes on Grid#2 were used for comparison purposes. As can be seen on both Fig. 4 and Table I, the method described in [4] suffers from errors, while the resonant frequencies almost overlap with the proposed method. The proposed method also compares favorably with an HFSS simulation of the same problem.

TABLE I
Resonant Frequencies of the Rectangular Resonator in GHz

Mode	HFSS	New method		Old method	
		Grid#1	Grid#2	Grid#1	Grid#2
1	1.8607	1.8605	1.8610	1.8812	1.8605
2	3.5474	3.5467	3.5467	3.5705	3.5700
3	4.9377	4.9386	4.9396	4.9521	5.0059
4	6.1882	6.1862	6.1862	6.1852	6.1665
5	7.5629	7.5600	7.5600	7.5641	7.6645

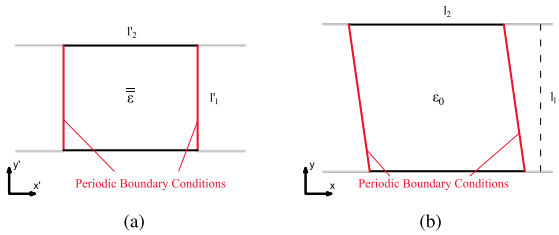

Fig. 5. (a) Original problem, a parallel-plate waveguide filled with anisotropy. (b) Dual problem, an empty parallel-plate waveguide with different dimensions.

B. Parallel-Plate Waveguide Filled With Anisotropic Material

The previous resonator example, unfortunately, did not have an analytical solution available to compare with the simulation. On the other hand, we were able to solve the resonant frequencies of a parallel-plate waveguide filled with anisotropic material analytically through transformation optics [10]. Transformation optics allows one to define a dual problem to the original one. In our case, the original problem was a parallel-plate waveguide with anisotropic material filling it. The dual was then defined as an empty parallel-plate waveguide with different dimensions (see Fig. 5) through a skew coordinate transformation. The propagating modes in both the original and the dual problem have the same frequencies, and the analytical solution is straightforward to find for the dual problem:

$$f_{mn} = \frac{c}{2\pi} \sqrt{\left(\frac{m\pi}{l_1}\right)^2 + \left(\frac{(\phi + n2\pi)}{l_2}\right)^2} \tag{13}$$

where c is the speed of light in free space, and ϕ is the phase difference between the periodic boundaries, and

$$a = \sqrt{\frac{1}{\epsilon_{yy}}}, \qquad l_1' = b l_1$$

$$b = \sqrt{\frac{\epsilon_{yy}}{\epsilon_{xx}\epsilon_{yy} - \epsilon_{xy}^2}}, \qquad l_2' = a l_2 .$$

As an example, the same anisotropic material as Section IV-A is chosen to be filling the waveguide. The width is $l_1' = 15$ mm, and $l_2' = 10$ mm. ϕ was also chosen to be 1 rad. This example was simulated with both HFSS and the proposed method, and compared with the analytical solution of (13). The Lebedev simulation was run at $\Delta x = \Delta y = 0.25$ mm for 120 000 time-steps. Also, to look at the order of accuracy for the Lebedev method, the same simulation was repeated with different mesh resolutions, and compared against the analytical solution to find the errors. Table II indicates that the proposed method agrees very well with both the analytic solution as well as HFSS

TABLE II
RESONANT FREQUENCIES OF THE PARALLEL-PLATE WAVEGUIDE IN GHZ

Mode	Analytical	Grid#1	Grid#2	HFSS
$f_{(0)(0)}$	1.8034	1.8036	1.8036	1.8034
$f_{(1)(0)}$	7.8425	7.8414	7.8414	7.8425
$f_{(0)(-1)}$	9.5277	9.5214	9.5214	9.5278
$f_{(1)(-1)}$	12.2208	12.1971	12.2012	12.2077
$f_{(0)(1)}$	13.1345	13.1172	13.1172	13.1351

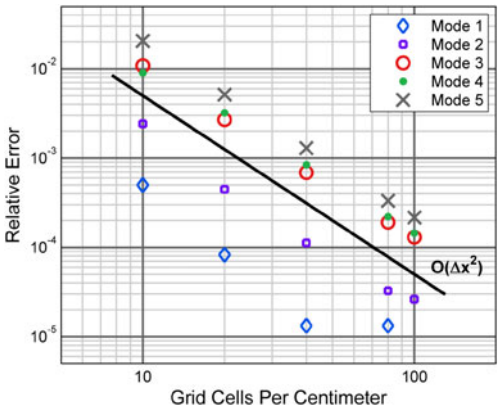

Fig. 6. Demonstration of second-order accuracy of Lebedev method in presence of planar PEC interfaces.

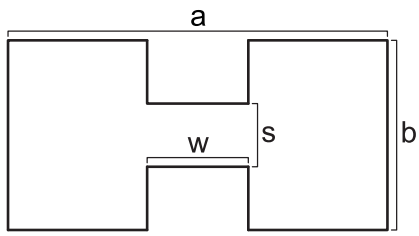

Fig. 7. Ridged resonator dimensions.

TABLE III
RESONANT FREQUENCIES OF THE RIDGED RESONATOR IN GHZ

Mode	HFSS	Grid#1	Grid#2
1	1.3197	1.3119	1.3211
2	3.6657	3.6653	3.6663
3	4.4565	4.4583	4.4555
4	6.1474	6.1455	6.1480
5	6.6634	6.6678	6.6590

simulations. Furthermore, Fig. 6 demonstrates the second-order accuracy of the algorithm for this example.

C. Ridged Resonator Filled With Anisotropic Material

To test the proposed method for the PEC corners, a ridged resonator was chosen as an example to cover all types of corners. The dimensions are $a = 30\,\text{mm}$, $b = 15\,\text{mm}$, $w = 8\,\text{mm}$ and $s = 5\,\text{mm}$ in Fig. 7. Again, filled with the same anisotropic material and mesh resolution of 0.25 mm. The results can be found on Table III. To investigate the order of accuracy, the simulation was run at different mesh resolutions, and the mesh resolution of $\Delta x = \Delta y = 0.1\,\text{mm}$ was chosen as the reference since there are no analytical solutions available. The simulated resonant frequencies agree very well with each other, as well as

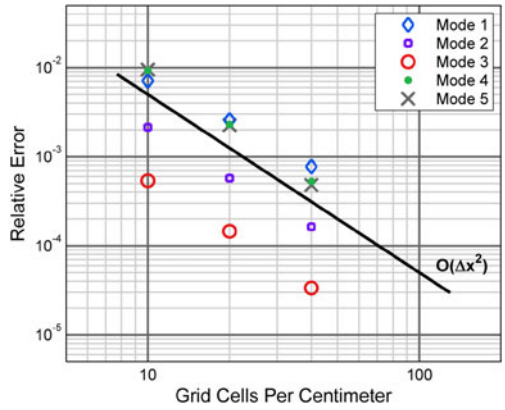

Fig. 8. Demonstration of second-order accuracy of Lebedev method in presence of PEC corners.

with HFSS simulations of the same structure. The second-order accuracy can be observed in Fig. 8.

V. CONCLUSION

The Lebedev-FDTD method was briefly overviewed followed by an explanation of errors in previous implementations of PEC surfaces in the method. The source of this error was found and corrected in our proposed method. Also, the PEC boundaries were generalized to include 270° corners. Several examples were provided to demonstrate the validity of the proposed techniques, and also show the second-order accuracy of this method in presence of PEC interfaces. Future work will include extending this method to three dimensions.

REFERENCES

[1] K. Yee, "Numerical solution of initial boundary value problems involving Maxwell's equations in isotropic media," *IEEE Trans. Antennas Propag.*, vol. AP-14, no. 3, pp. 302–307, May 1966.
[2] J. Schneider and S. Hudson, "A finite-difference time-domain method applied to anisotropic material," *IEEE Trans. Antennas Propag.*, vol. 41, no. 7, pp. 994–999, Jul. 1993.
[3] G. R. Werner and J. R. Cary, "A stable FDTD algorithm for non-diagonal anisotropic dielectrics," *J. Comput. Phys.*, vol. 226, no. 1, pp. 1085 –1101, 2007.
[4] M. Nauta, M. Okoniewski, and M. Potter, "FDTD method on a Lebedev grid for anisotropic materials," *IEEE Trans. Antennas Propag.*, vol. 61, no. 6, pp. 3161–3171, Jun. 2013.
[5] J. Liu, M. Brio, and J. V. Moloney, "An overlapping Yee finite-difference time-domain method for material interfaces between anisotropic dielectrics and general dispersive or perfect electric conductor media," *Int. J. Numer. Model.*, vol. 27, no. 1, pp. 22–33, 2014.
[6] C. Deimert, M. Potter, and M. Okoniewski, "Collocated electrodynamic FDTD schemes using overlapping Yee grids and higher-order hodge duals," *J. Comput. Phys.*, vol. 326, no. Supplement C, pp. 629–649, 2016. [Online]. Available: http://www.sciencedirect.com/science/article/pii/S0021999116304053
[7] I. V. Lindell, M. E. Ermutlu, K. I. Nikoskinen, and E. H. Eloranta, "Static image principle for anisotropic-conducting half-space problems; PEC and PMC boundaries," *Geophysics*, vol. 58, no. 12, pp. 1861–1864, 1993.
[8] C. J. Railton, I. J. Craddock, and J. B. Schneider, "Improved locally distorted CPFDTD algorithm with provable stability," *Electron. Lett.*, vol. 31, no. 18, pp. 1585–1586, Aug. 1995.
[9] X. Yuan, W. Y. Yin, X. H. Wang, J. Hu, and J. Jin, "Optimized conformal FDTD (2, 4) method for calculating reflected and diffracted electromagnetic fields of perfectly conducting wedges," *IEEE Trans. Electromagn. Compat.*, vol. 56, no. 2, pp. 466–474, Apr. 2014.
[10] D. H. Kwon and D. H. Werner, "Transformation electromagnetics: An overview of the theory and applications," *IEEE Antennas Propag. Mag.*, vol. 52, no. 1, pp. 24–46, Feb. 2010.